Laser-Driven Acceleration of Electrons in a Partially Ionized Plasma Channel

T. P. Rowlands-Rees,[1] C. Kamperidis,[2] S. Kneip,[2] A. J. Gonsalves,[1,*] S. P. D. Mangles,[2] J. G. Gallacher,[3] E. Brunetti,[3] T. Ibbotson,[1] C. D. Murphy,[4] P. S. Foster,[4] M. J. V. Streeter,[4] F. Budde,[5] P. A. Norreys,[4] D. A. Jaroszynski,[3] K. Krushelnick,[2] Z. Najmudin,[2] and S. M. Hooker[1]

[1]*University of Oxford, Clarendon Laboratory, Parks Road, Oxford OX1 3PU, United Kingdom*
[2]*Imperial College, Blackett Laboratory, Prince Consort Road, London SW7 2BW, United Kingdom*
[3]*University of Strathclyde, John Anderson Building, 107 Rottenrow, Glasgow G4 0NG, United Kingdom*
[4]*Rutherford Appleton Laboratory, Didcot, OX11 0QX, United Kingdom*
[5]*Friedrich-Schiller-University, PF 07737 Jena, Germany*

(Received 19 November 2007; published 14 March 2008)

The generation of quasimonoenergetic electron beams, with energies up to 200 MeV, by a laser-plasma accelerator driven in a hydrogen-filled capillary discharge waveguide is investigated. Injection and acceleration of electrons is found to depend sensitively on the delay between the onset of the discharge current and the arrival of the laser pulse. A comparison of spectroscopic and interferometric measurements suggests that injection is assisted by laser ionization of atoms or ions within the channel.

DOI: 10.1103/PhysRevLett.100.105005 PACS numbers: 52.38.Kd, 41.75.Jv, 52.38.Hb

In a plasma accelerator an intense laser or particle beam is used to drive a relativistic plasma wave, within which is formed a strong longitudinal electric field [1]. This field can be three or 4 orders of magnitude greater than that used in conventional accelerators, offering the prospect of a new generation of extremely compact accelerators with applications in both fundamental and applied science. The last few years have seen rapid progress in this area. Recently a particle-beam-driven plasma accelerator was used to double the energy of 42 GeV electrons in an 0.85 m long plasma [2]. A notable breakthrough in laser-driven plasma accelerators was reached in 2004 when quasimonoenergetic electron beams with energies of order 100 MeV were generated at plasma densities of order 10^{19} cm^{-3} by focusing intense laser pulses into helium gas jets [3,4] and in a plasma channel formed by additional laser pulses [5]. Increasing the output energy of a laser-driven plasma accelerator requires acceleration over a longer distance, and a lower plasma density than can be used with the guiding technique of [5]. These two requirements were first met in 2006 by guiding the driving laser pulses in a 33 mm long plasma channel formed by a hydrogen-filled capillary discharge waveguide [6,7], with a density of approximately 3×10^{18} cm^{-3}. Quasimonoenergetic electron beams with energies of 1 GeV were generated [8,9], which was the first demonstration of acceleration to beam energies comparable to those used in existing synchrotrons.

The mechanisms responsible for the generation of quasimonoenergetic beams by plasma accelerators driven in long plasma channels are complex, and presently the subject of several numerical studies. In this Letter we report the results of an experimental study of laser wakefield acceleration in a hydrogen-filled capillary discharge waveguide which provide new insights into the key process of injection of electrons into the laser wakefield. By combining measurements of the generated electron beams, the spectra of the transmitted laser radiation, and interferometric measurements of the plasma channel, we show that injection of electrons into the plasma wakefield is very likely to be assisted by ionization of partially-ionized species within the waveguide.

The hydrogen-filled capillary discharge waveguide has been described in detail elsewhere [6,7]. In these experiments 15 mm long sapphire capillaries of inner diameter $D = 200$ μm or 300 μm were employed. Hydrogen gas was flowed into the capillaries via channels of diameter 650 μm and length 10 mm located 4 mm from each end. A discharge was driven through the capillary by connecting across the capillary a 1.7 nF capacitor charged to a voltage (V) between 15 and 30 Kv. The discharge current was measured by a Rogowski coil.

The electron acceleration experiments were performed with the Astra Ti:sapphire laser at the Rutherford Appleton

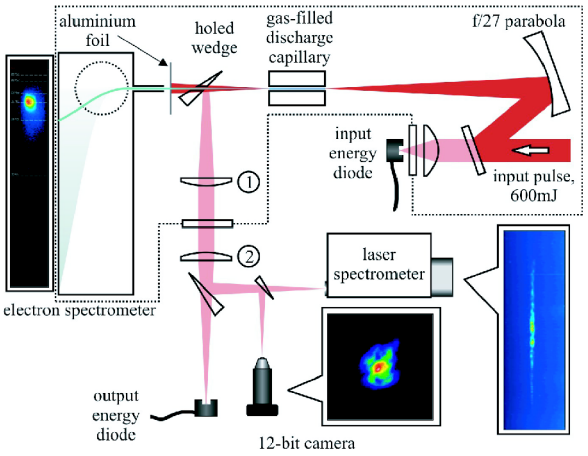

FIG. 1 (color online). Schematic diagram of the experiment. Elements within the dotted line were under vacuum.

Laboratory. The Astra laser delivered pulses with a mean wavelength of 818 nm and energy of 600 mJ. As illustrated in Fig. 1, the laser pulses were focused by an $f/27$ off-axis paraboloid to a waist of spot size 34 μm (radius of $1/e^2$ intensity) at the capillary entrance. The measured peak fluence at focus was 4×10^4 J cm^{-2}.

The delay t between the onset of the discharge current and the arrival of the laser pulse at the entrance of the waveguide was controlled by a digital delay generator. The timing jitter in t was measured to be less than 1 ns.

A portion of the laser radiation transmitted by the capillary was reflected by an optically flat wedge placed 0.6 m behind the capillary exit. After a second reflection from the surface of a wedge (not shown), the beam was collimated and refocused by two $f/15$ achromatic lenses to: (i) the entrance slit of a grating spectrometer; (ii) a 12-bit CCD, after magnification by a microscope objective. The spectral response of the imaging system and spectrometer was measured using a calibrated broadband source. The energies of the pulses entering and leaving the waveguide were measured by spectrally flat photodiodes behind a dielectric mirror prior to the paraboloid and behind a wedge after lens 2.

Electrons accelerated within the waveguide passed through a 4 mm diameter hole in the first wedge, were dispersed by a magnetic spectrometer, and recorded by a phosphor (Lanex) screen, imaged by a 12-bit CCD camera. Image plates were used to calibrate the measured signal to the charge of the electron bunch. Aluminium foils prevented laser radiation from entering the spectrometer.

The laser was operated in two distinct modes: a *short pulse* mode in which the laser was fully compressed to a pulse of full width at half-maximum (FWHM) duration 45 fs, corresponding to a peak intensity $I_{sp} = 8 \times 10^{17}$ W cm^{-2} and normalized vector potential $a_{0sp} = 0.60$; a *long pulse* mode in which a glass block prior to the compressor was removed, yielding pulses of 150 fs FWHM and a peak intensity $I_{lp} = 2.4 \times 10^{17}$ W cm^{-2}, corresponding to $a_{0lp} = 0.33$.

Experiments were performed using the short pulse for initial hydrogen pressures in the range 80 to 600 mbar. Quasimonoenergetic electron beams were observed with energies up to approximately 200 MeV and bunch charge of order 100 pC for capillaries with $D = 200$ μm, but no electron beams were observed for $D = 300$ μm.

A detailed study of the relation between guiding by the plasma channel and electron beam formation was undertaken. In order to show trends in the data for each set of data points $[y_i, t_i]$, we formed an averaged function $y(t)$ using a moving Gaussian window of full-width at half-maximum τ. We note that all data was collected with t varied randomly in order to counteract the effects of any drift in experimental parameters.

Figure 2(a) shows the averaged fractional laser energy transmission T for long and short laser pulses as a function

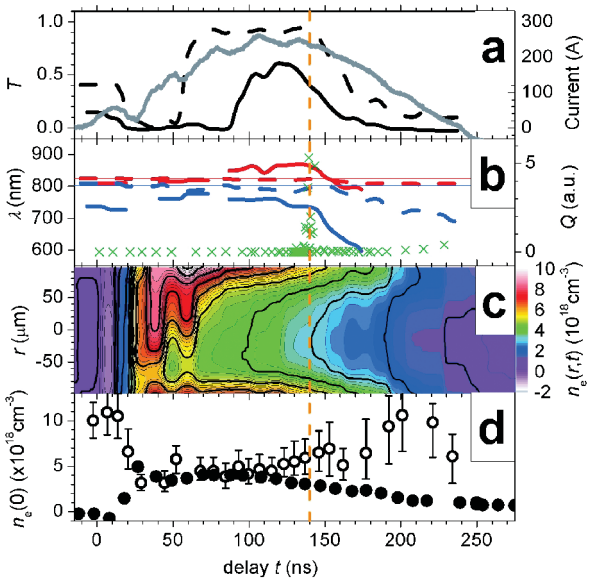

FIG. 2 (color). Measured data as a function of delay t for $D = 200$ μm, $P = 250$ mbar, $V = 25$ kV. (a) $T_{sp}(t)$ (solid black line), $T_{lp}(t)$ (dashed black line), and discharge current. (b) $\Lambda^{r,b}(t)$ for the short pulse (solid lines), long pulse (dashed lines), and input pulse (thin lines); and measured electron signal in arbitrary units, $[Q_i, t_i]$ (green crosses). (c) $n(r, t)$ (d) $[n_k^l, t_k]$ (solid dots); $[n_j^R, t_j]$ (hollow dots). All averaging was done with $\tau = 8.3$ ns. The delay time $t = 140$ ns is marked by the orange vertical dashed line.

of delay t. It is seen that for the long pulses T was approximately 0.95 for 70 ns $< t <$ 140 ns. Figure 3(b) shows the measured transverse fluence profiles in the exit plane of the waveguide for long pulses at several values of t in this range. The fact that T is high, and the transverse dimensions of the transmitted beams are comparable to the waist at the capillary entrance, shown in Fig. 3(a), demonstrates that a guiding channel is formed throughout this interval.

The behavior of the short pulses was distinctly different. As shown in Fig. 2(a) the peak energy transmission was only 0.6, consistent with deposition of energy into a plasma wave [8,9], and the range of delays for which the transmission was high was shorter. This behavior suggests that at the higher intensity of the short pulse, guiding was more sensitive to the state of the plasma channel, consistent with a stronger laser-plasma interaction. A stronger interaction may also explain the distortion of the fluence profiles shown in Fig. 3(c), although at these larger bandwidths (see below), chromatic aberration may contribute.

The spectra of the transmitted laser pulses may be characterized by defining a red(blue)-limit $\Lambda^r(\Lambda^b)$ for which 15.2% of the transmitted energy lies at longer (shorter) wavelengths. Figure 2(b) shows $\Lambda^{r,b}(t)$ for the long and short pulses. It is seen that for long pulses the red and blue limits of the spectra of the transmitted pulses are close to those of the input pulses throughout the interval in

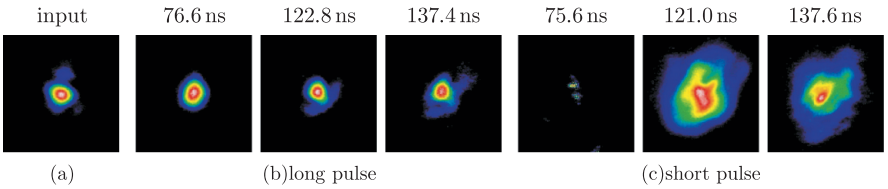

FIG. 3 (color online). Measured laser fluences from the data of Fig. 2: (a) in the entrance plane of the capillary; and in the exit plane of the capillary for long pulses (b) and short pulses (c). Each plot is 200 μm square and normalized to the maximum fluence of that shot.

which good guiding was observed. Again the short pulses behaved differently: strong, approximately symmetric broadening was observed even during the interval when the short pulses exhibited a high transmission. This observation is consistent with the short pulses driving a strong plasma wave, leading to significant spectral broadening by photon acceleration [10]. For longer delays, $t \gtrsim 140$ ns, the spectrum of the transmitted short pulse is both broadened and blueshifted.

Figure 2(b) also shows the measured electron charge $[Q_i, t_i]$ (in arbitrary units) for each short pulse shot. It is clear that electron beams were only generated for delays close to 140 ns. Figure 4 shows the measured peak electron energy (E_i, t_i) and the probability of injection $p(t)$, defined using the moving Gaussian average with $\tau = 1.7$ ns and $p_i = 1$ if a quasimonoenergetic electron beam was observed and $p_i = 0$ otherwise. The critical dependence on delay t is notable: of 13 shots in the range 130 ns $< t <$ 135 ns, none yielded electron beams; in contrast for 137 ns $< t <$ 141 ns 7 of 9 shots gave quasimonoenergetic beams. In this latter interval the mean and standard deviation of the electron beam energy were 128 and 15 MeV. We note that the peak probability $p(t)$ is 0.89 for $t = 139.8$ ns.

To gain further insight, interferometric measurements [11] of the plasma channel were performed on a capillary of square cross section with side 200 μm. Figure 2(c) plots the electron density $n(r, t)$ measured by interferometry for the same initial pressure and discharge conditions as used in the acceleration experiments. Good qualitative agreement between the channel shape and the behavior of the transmission of the long pulses shown in Fig. 2(a) is apparent. For delays less than 70 ns there is no well-defined channel and $T_{lp} \approx 0$. For $t > 70$ ns a channel forms and T_{lp} is high, and as the channel shape becomes symmetric T_{sp} also becomes high; at longer delays the depth of the channel decreases as do T_{lp} and T_{sp}.

The electron density near the axis of the channel could be measured in two ways: (i) interferometry yielded the axial electron density n^I directly; (ii) the spectra of the transmitted long pulses showed a distinct first Raman peak from which could be deduced an electron density. However, since the intensity of the leading edge of long pulses was sufficient to ionize partially-ionized species in the plasma channel, the electron density, n^R, deduced from the Raman shift corresponds to the sum of the densities of electrons ionized by the discharge and those ionized by the long laser pulse. Comparison of n^I and n^R therefore allows the degree of ionization of the channel to be estimated.

Figure 2(d) shows $[n_k^I, t_k]$ and $[n_j^R, t_j]$. At negative delays n_j^R is, within experimental error, equal to the density $(12 \times 10^{18}$ cm$^{-3})$ of hydrogen atoms at the initial pressure. It is seen that for 30 ns $\lesssim t \lesssim$ 120 ns, $n_k^I \approx n_j^R$, showing that the plasma channel is fully ionized. However, for longer delays $n_k^I < n_j^R$, indicating that the plasma channel is no longer fully ionized, although Figs. 2(a) and 3 show that the channel still acts as a waveguide at these delays. An effective degree of ionization in the axial region is given by n_k^I/n_j^R; at the critical delay for electron injection ($t \approx 140$ ns) this is equal to 0.5 ± 0.2.

The results presented above demonstrate clearly that in these experiments the generation of quasimonoenergetic electron beams required the presence of a plasma channel. Electron beams were not observed for negative delays, when the laser interacted with neutral gas. Interferometric measurements showed that a plasma channel was formed at delays t for which electron beams were generated, as confirmed by the observed high-quality channelling of the long pulse. Finally, electron beams were not generated for capillaries with $D = 300$ μm, but were for $D = 200$ μm suggesting that injection and acceleration required a sufficiently small matched spot size of the channel, which varies as $D^{0.651}$ [11].

The sensitivity of the generation of electron beams to the delay t is striking. Interferometry and the long pulse guiding data show that a plasma channel was formed for a

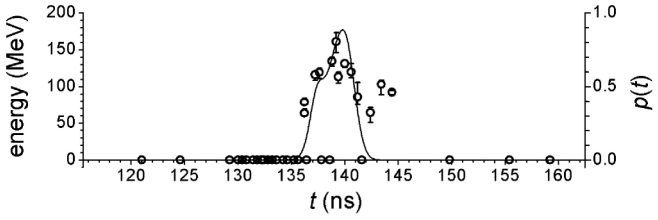

FIG. 4. Electron energy (circles) and $p(t)$ (line) as a function of t from the data of Fig. 2. The energy is taken to be zero for shots in which no electrons were observed.

duration of at least 70 ns; broadening of the spectrum of the transmitted short pulse, indicating strong wakefield formation, occurred over an interval of 50 ns; but electron beams were only observed for a range of delays approximately 5 ns wide.

It is clear, therefore, that electron injection depends sensitively on the state of the plasma channel—i.e., to the transverse and longitudinal density profile, and its degree of ionization. With regard to the latter, Fig. 2(d) shows that on axis the channel was fully ionized for a period of approximately 90 ns, but at the delay for which electrons were generated the plasma was not fully ionized. We note that this delay also coincides with the onset of a strong blueshift of the spectrum of the transmitted short pulse, consistent with transmission through a partially ionized channel. The results presented here strongly suggests that the sensitivity of injection to the delay t arises from the dual requirement that a plasma channel is formed and that near the axis the plasma is not fully ionized.

Several mechanisms could be responsible for a dependence of injection on the degree of ionization. Recently it was shown that the electrons injected and accelerated in a particle-beam driven plasma accelerator originated from field ionization of He^+ within the wakefield [12]. That work showed that the generation of electrons within the wakefield reduced the threshold for trapping since they may be born with zero velocity at phases for which the electrons of the background plasma have significant backwards momentum. The results presented in the present paper might be explained by an analogous process occurring in a laser-driven plasma accelerator. We note that ionization could also promote electron injection by the increased ponderomotive force at an ionization front [13] or by plasma heating.

There are two possible sources of partially ionized species: Al and O from the Al_2O_3 wall, and recombined hydrogen. The threshold intensities for above-barrier ionization are: 0.59, 1.0, 1.3 and 530×10^{18} W cm^{-2} for Al^{n+}, $n = 8$–11; 0.04 and 25×10^{18} W cm^{-2} for O^{n+}, $n = 5$ and 6; 1.4×10^{14} W cm^{-2} for H. It is clear that any Al or O ions present near the axis of the channel would be ionized near the peak of the laser pulse, and hence within the plasma wakefield. It might be expected that neutral hydrogen would be ionized well outside this region. However strong steepening of the laser pulse, and lower than expected ionization rates at high intensities [14,15], could allow sufficient H atoms to survive close to the peak of the laser pulse. We note that the required density of species donating electrons is low: if injection occurs in a volume at least equal to the plasma wavelength cubed, a 100 pC electron bunch corresponds to a donor density of less than 3% of the axial plasma density.

It is worth emphasizing that, although narrow, the range of delays for electron injection occurred was greater than the experimental jitter, allowing electron beams to be generated with approximately 90% probability. Further, the electron energies achieved with a plasma waveguide were approximately double those obtained using a helium gas jet with the same laser [3]. This observation is consistent with the fact that the use of a plasma channel allows injection and acceleration over a distance of order the dephasing length at lower plasma densities.

In summary, we have generated quasimonoenergetic electron beams with energies up to 200 MeV with a laser plasma accelerator driven in a hydrogen-filled capillary discharge waveguide. Electron beams were only generated under conditions in which a plasma channel was formed. Injection and acceleration of electrons was found to depend sensitively on the delay t between the onset of the discharge current and the arrival of the laser pulse but, importantly, to be highly reproducible. A comparison of spectroscopic and interferometric measurements allowed the degree of ionization of the plasma channel to be determined for the first time, and strongly suggest that in these experiments injection was assisted by laser-ionization of atoms or ions within the channel. This injection process could be enhanced by employing mixtures of hydrogen and other gasses which would not be fully ionized by the discharge, allowing control of the density and position relative to the wakefield of the laser-ionized electrons. The results presented here could therefore open a new route for controlling the electron injection process, and hence increase the shot-to-shot stability of the energy, pointing, and charge of laser-accelerated electron beams to the levels required for applications.

The authors acknowledge invaluable discussions with R. Trines, and with W. P. Leemans and his group; and are grateful for technical assistance from C. J. Woolley, K. O'Keeffe, and the staff at Rutherford Appleton Laboratory. S. P. D. M. acknowledges support from the Royal Society. This work was funded by the RCUK via Grant No. GR/R88090.

*Present address: Lawrence Berkeley National Laboratory, Berkeley, CA, USA.

[1] T. Tajima *et al.*, Phys. Rev. Lett. **43**, 267 (1979).
[2] I. Blumenfeld *et al.*, Nature (London) **445**, 741 (2007).
[3] S. P. D. Mangles *et al.*, Nature (London) **431**, 535 (2004).
[4] J. Faure *et al.*, Nature (London) **431**, 541 (2004).
[5] C. G. R. Geddes *et al.*, Nature (London) **431**, 538 (2004).
[6] D. J. Spence *et al.*, Phys. Rev. E **63**, 015401 (2000).
[7] A. Butler *et al.*, Phys. Rev. Lett. **89**, 185003 (2002).
[8] W. P. Leemans *et al.*, Nature Phys. **2**, 696 (2006).
[9] K. Nakamura *et al.*, Phys. Plasmas **14**, 056708 (2007).
[10] C. D. Murphy *et al.*, Phys. Plasmas **13**, 033108 (2006).
[11] A. J. Gonsalves *et al.*, Phys. Rev. Lett. **98**, 025002 (2007).
[12] E. Oz *et al.*, Phys. Rev. Lett. **98**, 084801 (2007).
[13] W. B. Mori *et al.*, Phys. Rev. Lett. **69**, 3495 (1992).
[14] B. B. Wang *et al.*, Chin. Phys. Lett. **23**, 2729 (2006).
[15] J. Gorlinger *et al.*, Appl. Phys. B **71**, 331 (2000).